HiSST: 3rd International Conference on
High-Speed Vehicle Science Technology
14 -19 April 2024, Busan, Korea

Heat Transfer to a Flat Plate under Partially Dissociated Nitrogen Freestream Condition

Guangjing Ju [1], Lin Bao [2]

Abstract

This research focuses on the impact of chemical non-equilibrium on heat transfer in high-enthalpy shock tunnel experiments. The rapid acceleration of the expansion flow originating from the high-temperature chamber leads to thermochemical non-equilibrium and incomplete wall catalysis. Consequently, understanding these effects is crucial for accurate heat transfer measurements. Employing computational fluid dynamics, this study investigates the influence of partially catalytic walls on heat flux under high-enthalpy shock tunnel conditions, utilizing a flat plate model. We propose a division of wall heat flux into two components: one governed by classical boundary layer theory, associated with translational-rotational energy, and the other determined by the Damköhler number, linked to catalytic reactions. These findings contribute to developing a methodology for ground-to-flight extrapolation in chemical non-equilibrium hypersonic flows.

Keywords: *hypersonic shock tunnels, chemical nonequilibrium, catalytic surface effects*

Nomenclature

Latin
Da – Damköhler number
M – Mach number
Re_L – unit Reynolds number
q – heat flux
T – temperature

Greek
α – degree of dissociation
γ_{cat} – catalytic coefficient

Subscripts
c – catalytic reaction
e – outer edge of the boundary layer
r – recombination
tr – translational
v – vibrational
VT – vibrational-translational
w – wall
∞ – freestream

1. Introduction

Shock tunnels, like LENS [1], play a crucial role in studying hypersonic aerodynamics and aerothermodynamics. In high-enthalpy experiments, gas molecules in the shock tube's reservoir become highly excited, leading to non-equilibrium conditions in the freestream over the test model [2,3]. This non-equilibrium state, characterized by low translational and rotational temperatures but high vibrational temperatures and gas dissociation, results in real gas effects in hypersonic flow [3,4].

Surface catalytic recombination further influences aeroheating, contributing a substantial portion of the total heat flux. Gas-surface interactions and catalytic recombination reactions on the wall play a role in transferring energy to the wall and inducing catalytic heating. Studies have shown that catalytic heating

[1] *University of Chinese Academy of Sciences, Address No.19A Yuquan Road, Shijingshan District, Beijing 100049, China, juguangjing22@mails.ucas.ac.cn*
[2] *University of Chinese Academy of Sciences, Address No.19A Yuquan Road, Shijingshan District, Beijing 100049, China, lbao@ucas.ac.cn*

can account for a significant portion of the total heat flux in shock tunnel experiments [5].Despite previous research on flat plate models [2,6], a comprehensive quantitative description of aero-heating under the combined effects of thermochemical nonequilibrium flow and incomplete catalysis is lacking.

In this study, we use computational fluid dynamics to investigate the impact of catalytic nonequilibrium on heat transfer to a flat plate in a partially dissociated hypersonic nitrogen freestream. Then we develop a formula based on the criterion to estimate heat flux in partially dissociated freestream conditions.

2. Model and Theoretical analysis

2.1. Model and freestream conditions

In this study, we focus on the flat plate model as it is one of the most fundamental models both in experiments and in numerical studies. The length of the flat plate shown in Fig 1 is chosen to match the model in the real shock tunnel experiments [7]. Free-stream condition in group D1 is consistent with the thermochemical nonequilibrium experimental condition in Ref. [8]. Freestream conditions are modified in Group A, Group B and Group C to further investigate the relation of heat flux and surface catalysis by changing the Mach number, Reynolds number and the degree of dissociation. The catalysis coefficient γ is successively set to 0, 0.001, 0.01, 0.1 and 1.

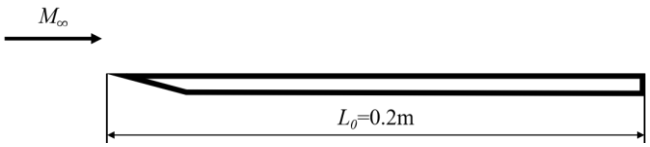

Fig 1. Schematic of a hypersonic flow over a sharp leading-edge flat plate

Under the freestream conditions mentioned in Table1, only translational, rotational, and vibrational mode energy of the particles is excited. The relaxation time of the translational and rotational energy is recognized as impractically short [9]. Therefore, it is practical to employ two temperature model in the present study.

Table 1. Freestream conditions considering thermochemical nonequilibrium and wall catalysis

Case	M_∞	$Re_{L,\infty}$	T_{tr} (K)	T_v (K)	α_∞	γ_{cat}	Da_{VT}	Da_r
A1	8	2.0E5	800	4700	10%	0~1	8.0E-5	3.6E-5
A2	10	2.0E5	800	4700	10%	0~1	5.1E-5	1.8E-5
A3	12	2.0E5	800	4700	10%	0~1	3.5E-5	1.1E-5
B1	8	8.0E4	800	4700	10%	0~1	3.2E-5	5.7E-6
B2	8	2.0E5	800	4700	10%	0~1	8.0E-5	3.6E-5
B3	8	4.0E5	800	4700	10%	0~1	1.6E-5	1.4E-4
C1	8	2.0E5	800	4400	5%	0~1	8.0E-5	3.6E-5
C2	8	2.0E5	800	4700	10%	0~1	8.0E-5	3.6E-5
C3	8	2.0E5	800	5000	15%	0~1	8.0E-5	3.6E-5
D1	6.94	2.7E5	1342	4715	10%	0~1	3.5E-03	1.8E-04

The degree of vibrational-translational (V-T) energy transfer nonequilibrium can be described by:

$$Da_{\mathrm{VT}} = \frac{\tau_{\mathrm{f}}}{\tau_{\mathrm{V}}} \tag{1}$$

where $\tau_{\mathrm{f}} = \mathrm{L}_0/\mathrm{u}_\infty$ is the characteristic time of flow over the model surface, and τ_{V} is the characteristic time of the V-T energy transfer, which can be estimated by Landau-Teller model [10]:

$$\tau_{\mathrm{v}} = \frac{c_1}{p_\infty}\exp\left[\left(\frac{c_2}{T_{\mathrm{tr}}}\right)^{\frac{1}{3}}\right] \tag{2}$$

where p_∞ is the free-stream pressure and $C_1 = 7.12 \times 10^{-3}\mathrm{atm}\cdot\mu\mathrm{s}$, $C_2 = 1.91 \times 10^{6}\mathrm{K}$ can be obtained from Ref. [11].

The nonequilibrium degree of recombination can be described by nonequilibrium criterion Da_r, which is written as

$$Da_r = \frac{\tau_f}{\tau_r} \tag{3}$$

where the characteristic time of recombination reactions in the boundary layer $\tau_r = [N]/v_{chem}$, and $[N]$ is the concentration of Nitrogen atom, and v_{chem} can be estimated by the chemical kinetics model by Park's model [12].

Presented in Fig 2 is the microscopic process of catalytic recombination (Eley–Rideal mechanism, for example), homogeneous collision and possible diffusion. In this figure, γ_{cat} is the catalytic coefficient, represents the probability of the catalytic reaction when an atom collides with the wall. In this study, the effects of chemical and vibrational energy accommodation are not included.

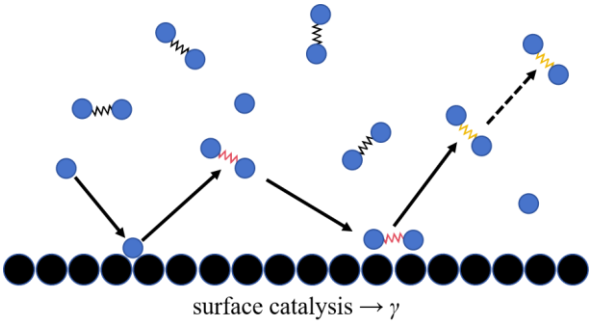

Fig 2. Schematic of the gas-surface interaction

2.2. Governing equation

Since we do not consider the chemical reactions in the flow field, the source term and chemical reaction related term are omitted. The governing equations are similar to Prandtl's boundary-layer equations:

$$\begin{cases} \dfrac{\partial(\rho u)}{\partial x} + \dfrac{\partial(\rho v)}{\partial y} = 0; \\ \rho u\dfrac{\partial u}{\partial x} + \rho v\dfrac{\partial u}{\partial y} = -\dfrac{dp_e}{dx} + \dfrac{\partial}{\partial y}\left(\mu\dfrac{\partial u}{\partial y}\right); \\ \dfrac{\partial p}{\partial y} = 0; \\ \rho u\dfrac{\partial h_{tr}}{\partial x} + \rho v\dfrac{\partial h_{tr}}{\partial y} = \dfrac{\partial}{\partial y}\left(k\dfrac{\partial T_{tr}}{\partial y}\right) + u\dfrac{dp_e}{dx} + \mu\left(\dfrac{\partial u}{\partial y}\right)^2; \\ \rho u\dfrac{\partial c_i}{\partial x} + \rho v\dfrac{\partial c_i}{\partial y} = \dfrac{\partial}{\partial y}\left(\rho D\dfrac{\partial c_i}{\partial y}\right). \end{cases} \tag{4}$$

where u and v are x and y component of velocity respectively, ρ is the density, h is the enthalpy, c_i is the concentration of specie i, μ is the viscosity coefficient, k is the thermal conductivity, D is the diffusivity. The subscript e and w denote the properties at the outer edge of the boundary layer and at the wall, respectively.

Compared with compressible boundary-layer equations with no chemical reactions, we find out that this set of equations with finite-rate catalytic boundary condition also has self-similar solutions.

The compressible boundary-layer equation can be solved by introducing Lees-Dorodnitsyn transformation:

$$\begin{cases} \xi = \int_0^x \rho_e u_e \mu_e dx \\ \eta = \dfrac{u_e}{\sqrt{2\xi}}\int_0^y \rho dy \end{cases} \tag{5}$$

Define dimensionless velocity, enthalpy and concentration as follows:

$$\begin{cases} \frac{u}{u_e} = \frac{\partial f}{\partial \eta} \equiv f'; \\ \frac{h}{h_e} = g; \\ \frac{c}{c_e} = z. \end{cases} \tag{6}$$

By making cold wall assumption ($\mathrm{T_w} \ll \mathrm{T_e}$) and assuming Chapman-Rubesin factor $\mathrm{C} = \rho\mathrm{u}/\rho_\mathrm{e}\mathrm{u}_\mathrm{e} = 1$ and Schmidt number $\mathrm{Sc} = \mathrm{const.}$, the conservation equations are thus transformed into:

$$\begin{cases} f''' + ff'' = 0; \\ g'' + Prfg' = 0; \\ z'' + Scfz' = 0. \end{cases} \tag{7}$$

This set of equations are identical to the traditional boundary layer equations except for the additional equations of non-dimensional enthalpy and concentration. Therefore, we can get the theoretical solutions after deduction of the boundary conditions.

2.3. The catalytic boundary condition

From Fick's law, the mass flux to the wall is:

$$j = \rho_w D_w \left(\frac{\partial c}{\partial y}\right)_w \tag{8}$$

Considering conservation of mass at the wall and the first-order catalytic reaction, the diffusion flux to the surface is equal to the loss caused by chemical reaction:

$$\rho_w D_w \left(\frac{\partial c}{\partial y}\right)_w = k_w \rho_w c_w \tag{9}$$

Therefore, the finite-rate catalytic wall boundary condition is:

$$\left(\frac{\partial c}{\partial y}\right)_w = k_w c_w / D_w = \frac{k_w \rho_w c_w}{Sc \mu_w} \tag{10}$$

Therefore, the boundary conditions after similarity transformation are:

$$\begin{cases} f(0) = f'(0) = 0, f'(\infty) = 1; \\ g(0) \ll 1 (T_w \ll T_e), g(\infty) = 1; \\ z'(0) = (2Re_{x,e})^{1/2} \frac{\mu_e}{u_e} \frac{Sc}{\mu_w} k_w z(0), z(\infty) = 1. \end{cases} \tag{11}$$

2.4. Theoretical solution and prediction of heat flux to the wall

The theoretical solution to Eq. (7) is:

$$\begin{cases} f''(0) = \frac{0.664}{\sqrt{2}} = 0.47; \\ g'(0) = \sqrt{2}(0.664) Pr^{1/3} = 0.47 Pr^{1/3}; \\ z(0) = \frac{1}{1 + (2Re_{x,e})^{1/2} \frac{\mu_e}{u_e} \frac{Sc}{\mu_w} k_w \frac{1}{0.47 Sc^{1/3}}}. \end{cases} \tag{12}$$

Our previous investigation has modeled the incomplete accommodation of vibrational energy on vibrationally excited hypersonic flow over flat plate [2]. The similarity between these two problems, the incomplete accommodation of the vibrational energy and the partial catalysis of heterogeneous reactions, are significant. Because both of them are results from the energy transfer from the gas particles to the wall, the nonequilibrium mechanism can be modeled in the same framework. The chemically frozen flow and catalytic problems have been comprehensively studied, and useful theories [13,14] have been established. Therefore, we can avoid repetitive deductions, and directly acquired the results based on analogy method.

The key parameter α_w, denoting the degree of dissociation at wall, can be obtained by:

$$\frac{\alpha_\mathrm{w}}{\alpha_\mathrm{e}} = \frac{1}{1 + Da_\mathrm{c}} \tag{13}$$

where subscript "e" and "w" denotes the value at the outer edge of the boundary-layer and at wall respectively and $\mathrm{Da_c}$ is the specific Damköhler number for the catalysis nonequilibrium of heterogeneous reactions. $\mathrm{Da_c}$ is introduced as:

$$Da_{\mathrm{c}} = A\frac{Re_{\mathrm{x,e}}^{1/2}}{Ma_{\mathrm{e}}}\left(\frac{T_{\mathrm{tr,e}}}{T_{\mathrm{w}}}\right)^{1/2}\gamma_{cat}\ ,A = \frac{Sc^{2/3}}{0.332\sqrt{2\pi\gamma}} \tag{14}$$

where A is a constant related to gas properties, γ is the specific heat of overall gas. Considering the effects of viscous interaction and assuming values at the outer edge of the boundary-layer equals to the values at infinity, we obtain an approximate but practical transfiguration of Eq. (14)

$$Da_{\mathrm{c}} = A\chi\frac{Re_{\mathrm{x,\infty}}^{1/2}}{Ma_{\infty}}\left(\frac{T_{\mathrm{tr,\infty}}}{T_{\mathrm{w}}}\right)^{1/2}\gamma_{cat} \tag{15}$$

where χ is introduced to represents a correction for the viscous interaction effects [7], which is written as:

$$\chi = \sqrt{\frac{p_{\mathrm{w}}}{p_{\infty}}} = \sqrt{1 + 0.332(\gamma - 1)\left(1 + 2.6\frac{T_{\mathrm{w}}}{T_{\mathrm{tr,0}}}\right)\bar{\chi}} \tag{16}$$

where γ is the specific heat of overall gas, and for the sake of convenience $\gamma \approx 1.4$, $\mathrm{T_{tr,0}} = \mathrm{T_{tr,\infty}}[1 + 0.5(\gamma - 1)\mathrm{Ma}_{\infty}^{2}]$ is the total temperature converted from freestream $\mathrm{T_{tr}}$, $\bar{\chi} = Ma_{\infty}^{3}\sqrt{C^{*}/Re_{\mathrm{x,\infty}}}$ is the viscous interaction parameter, and $\mathrm{C}^{*} = \rho^{*}\mu^{*}/(\rho_{\infty}\mu_{\infty})$ represents the influences of the nonlinear viscosity-temperature law in the high temperature flows, where superscript "$*$" refers to the values at reference temperature [11].

Specifically, for dissociated nitrogen and a cold wall condition, there are two limitations. First, as $\gamma_{\mathrm{cat}} \to 0$, $\mathrm{Da_c} \to 0$, Eq. (15) indicates that the gas composition is nearly identical compared to the freestream composition and the catalytic reactions can be regarded as frozen. On the contrary, as $\gamma_{cat} \to 1$, $\mathrm{Da_c} \to \infty$, the dissociation degree at wall $\alpha_{\mathrm{w}} \to 0$, and the heterogeneous reactions could be regarded as equilibrium. Hence, $\mathrm{Da_c}$ is considered as a specific Damköhler number defined by the ratio of the characteristic time scale of the flow to that of the heterogeneous reactions and it indicates the nonequilibrium degree of catalysis effect.

The heat conduction of translational-rotational energy through the hypersonic flat plate flow boundary-layer to model surface is directly proportional to the difference of the thermal or frozen enthalpy at the outer edge of the boundary-layer and that at the wall. Namely, $\mathrm{q_{tr}}$ can be expressed as

$$q_{\mathrm{tr}} = St_{\mathrm{tr}}\rho_{\infty}V_{\infty}\left(h_{\mathrm{tr,aw}} - h_{w}\right) \tag{17}$$

where $\mathrm{h_{tr,aw}}$ is the adiabatic-wall specific enthalpy without vibrational degree of freedom, and $\mathrm{h_w}$ is the wall specific enthalpy, and $\mathrm{St_{tr}}$ is the Stanton number for $\mathrm{q_{tr}}$.

Similarly, the catalytic heating can be written as

$$q_{\mathrm{c}} = St_{\mathrm{c}}\rho_{\infty}V_{\infty}(\alpha_{\mathrm{e}} - \alpha_{w})R\theta_{\mathrm{d}} = St_{\mathrm{c}}E_{\mathrm{d}}(\alpha_{\mathrm{e}} - \alpha_{w}) \tag{18}$$

where $\mathrm{E_d} = \rho_{\infty}\mathrm{V_{\infty}R\theta_d}$ representing the dissociation energy for nitrogen, and R is the specific gas constant, and $\theta_{\mathrm{d}} = 101325\mathrm{K}$ is the characteristic dissociation temperature of nitrogen. The $\mathrm{St_c}$ only differs from the $\mathrm{St_{tr}}$ by the replacement from Prandtl number to the Schmidt number. $\mathrm{St_c/St_{tr}} = (\mathrm{Pr/Sc})^{-0.6} = \mathrm{Le}^{-0.6}$, where Le is Lewis number, and the value of the Lewis number is best estimated to be 0.6 [15]. As a result, the total heat flux to the flat plate is

$$q_{\mathrm{w}} = q_{\mathrm{tr}} + q_{\mathrm{v}} + q_{\mathrm{c}} \tag{19}$$

where $\mathrm{q_{tr}}$ can be obtained by classical boundary-layer theory and $\mathrm{q_v}$ can be determined by our previous work [2], and $\mathrm{q_c}$ is given as

$$q_{\mathrm{c}}/q_{\mathrm{tr}} = Le^{-0.6}\frac{\alpha_{\mathrm{e}}}{\tilde{\mu} - \alpha_{\mathrm{e}}}\frac{Da_{\mathrm{c}}}{1 + Da_{\mathrm{c}}} \tag{20}$$

where $\alpha_{\mathrm{e}} \approx \alpha_{\infty}$, and $\tilde{\mu} = \mathrm{E_{\infty}/E_d} \approx \mathrm{V_{\infty}^2/(2R\theta_d)}$. It is clear from Eq. (20) that the heat flux is mainly determined by the freestream dissociation degree (α_{∞}) and the degree of wall catalysis nonequilibrium ($\mathrm{Da_c}$).

3. Solver and Numerical Methods

3.1. A brief on the solver

The full name of the solver used in this study is NNW-HyFLOW, which is referred to as the HyFLOW software in this paper. HyFLOW software is developed on the basis of the PHengLEI open source software [16,17], and it shows high efficiency, good computational reliability and numerical stability[18]. The solver is based on the structure grid finite volume method and it can solve both steady and unsteady problems. More detailed information of HyFLOW and will be introduced in the following sections and can be found in literature [19,20].

3.2. Physical and chemical model

For thermochemical nonequilibrium gas, the pressure of the mixture gas is calculated by the Dalton's law of partial pressures, while other thermodynamic state parameters are calculated by equation of state for the ideal gas. The thermodynamic parameters such as internal energy, specific heat and enthalpy are calculated using the model of molecular kinetic theory. The viscosity and thermal conductivity and are calculated using the Blottner's fitting formula and Eucken's empirical formula respectively. The mass diffusivity is calculated by the method based on the assumption of constant Schmidt number, and the Wilke's mixing law is used to calculate the transport parameters of the mixture gas.

The vibrational energy transport term is calculated by the Landau-Teller formula, and the translation-vibration relaxation time indicates the sum of the Millikan-White time and the Park correction time. The HyFLOW software integrates common chemical reaction models such as Gupta, Dunn-Kang and Park, in which both the forward and reverse reaction rates are estimated by the Arrhenius formula. Since the temperature region we consider is not high enough to let the air ionized, we employ Park's 5 species air model [12] for all cases. Considering the thermochemical coupling effect, the control temperature of the forward and reverse reaction rates is corrected by the Park's vibration-dissociation coupling model:

$$T_c = T^a T_v^{1-a} \tag{21}$$

where the exponent of translational temperature is assigned with the default value of a = 0.6.

For gas-surface interactions, the HyFLOW software includes non-catalytic wall, fully catalytic wall and finite-rate catalytic wall. The reaction rate at the wall k_w is calculated by:

$$k_w = \gamma_{cat}\sqrt{\frac{RT_w}{2\pi \mathrm{M}_r}} \tag{22}$$

where γ_{cat} is the catalytic efficiency or recombination coefficient, R is the universal gas constant, T_w is the wall temperature and M_r is the molar mass of the reactant. Consider the mass conservation on the surface:

$$\dot{m} = -\rho D\ (\nabla c \cdot n) \tag{23}$$

where D is the diffusivity. Therefore, the molar mass fraction of the species on the surface is determined.

3.3. Numerical methods

The equations are discretized using the time first-order backward difference scheme and the Steger-Warming vector flux splitting method, and the LU-SGS iterative scheme is used for calculation. In addition, the nonequilibrium source term is handled with the point implicit method by default in the HyFLOW software. The HyFLOW flux schemes such as Roe, Steger and AUSM class, as well as common limiters such as Vanleer, Minmod, Vanalbada, etc. In a nutshell, the solver is first-order accurate in time domain and second-order accurate in spatial domain.

In this study, we chose the steady-state laminar flow solver and use Steger-Warming discretization and Minmod limiter for numerical simulation. The iteration number is first set to a large number, and we stop computing when the solution is converged.

3.4. Verification on the solver and grid independence study

The solver has been verified and validated for hypersonic aero-heating calculations and has exhibited favorable agreement with results obtained from the LENS experiments and the DPLR code [20]. To

further verify the finite-rate catalytic wall boundary condition in HyFLOW, we chose the Run 77 case from a recent experiment by Maclean [21] and the freestream conditions are shown in Table 2, identical to the literature. As shown in Fig 3, the numerical results are in good agreement with both the experiment result and the numerical results calculated with DPLR code from the literature. Therefore, the catalytic wall boundary condition is functional in HyFLOW.

Table 2. Freestream conditions for the verification case

M_∞	$Re_\infty(m^{-1})$	$T_\infty(K)$	$T_w(K)$	Gas Model
17.9	3.4e5	156	300	Air (2T, Park)

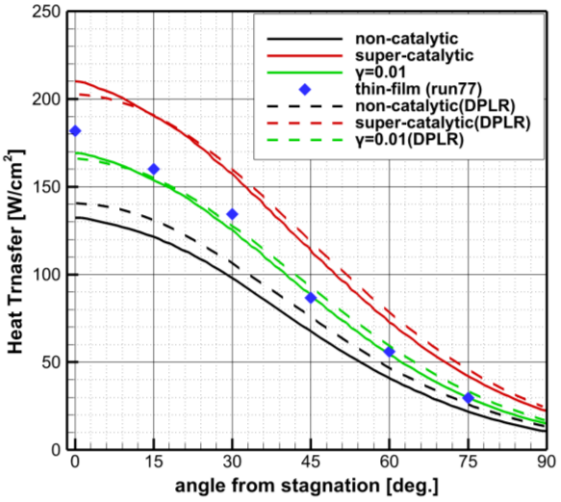

Fig 3. Heat transfer to the wall for hypersonic flow over a cylinder

The boundary conditions are specified as follows. The free-stream conditions given in Table 1 are set as the inflow boundary; the no-slip and isothermal finite-rate catalytic wall is employed on the surface of the plate because the wall temperature of the model remains nearly constant in experiments due to the very short run time of the tunnel. The outlet is supersonic outlet, considering the flow after the shock is still supersonic under the free-stream condition in this study.

The structure of the computational grid is illustrated for clarity in Fig 4, with grid refinement near the leading edge and surface of the plate. To calculate the surface heat flux correctly, the wall cell Reynolds number should be smaller than 3 [22]. Therefore, the scale of the first layer normal to the surface is set to 10^{-6}m to let the wall cell Reynolds number smaller than 1 for all cases. A grid-independence study was carried out as an example for condition D1 from Table 1 with three refinement levels: 120×140 (coarse), 200×200 (medium), and 300×300 (fine). The grid-independence study is shown in Fig 5, and both the heat flux due to surface catalysis and translational-rotational energy are almost identical for different grids. Thus, the medium level of refinement is sufficient.

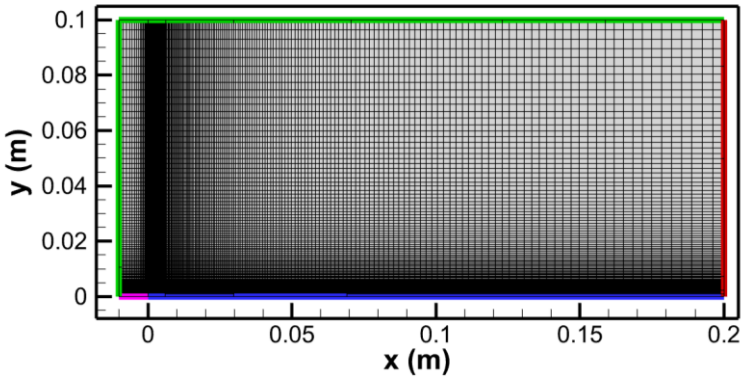

Fig 4. Schematic of computational grid structure.

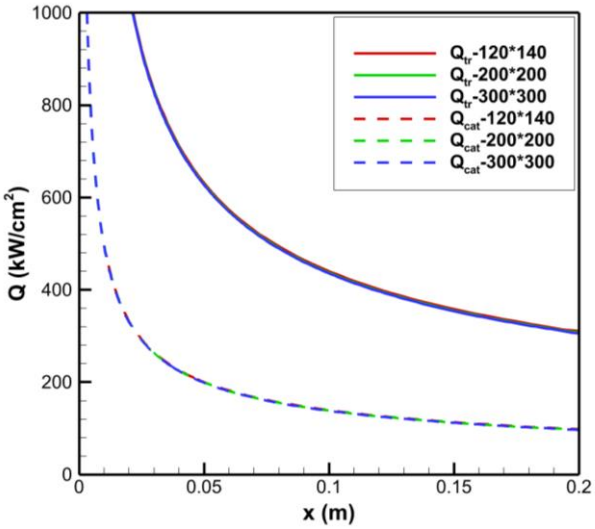

Fig 5. Grid-independence verification for heat transfer along the plate (case D1).

4. Results and discussion

A series of simulations using condition D1 with wall catalytic coefficient successively set to 0, 0.001, 0.01, 0.1, 1 are conducted to investigate the nonequilibrium degree of V-T energy transfer and homogeneous reactions. The numerical results are presented in Fig 6. The distribution of the translational-rotational temperature profiles is almost identical even though the surface catalysis is different. The distribution of the dissociation degree $\alpha = \mathrm{N_d}/\mathrm{N_{tot}}$, where $\mathrm{N_d}$ is the number of dissociated molecules and $\mathrm{N_{tot}}$ being total number of original molecules, varies with the wall catalytic coefficient while translational-rotational temperature remains almost unchanged. In other words, the chemical reactions in the gas phase are frozen. For the remained cases, the translational-rotational temperature and dissociation degree profiles have the same characteristic as that in D1. Therefore, we can conclude that all cases in this study satisfy the assumption that the V-T energy transfer and the chemical reactions in the gas phase are both frozen.

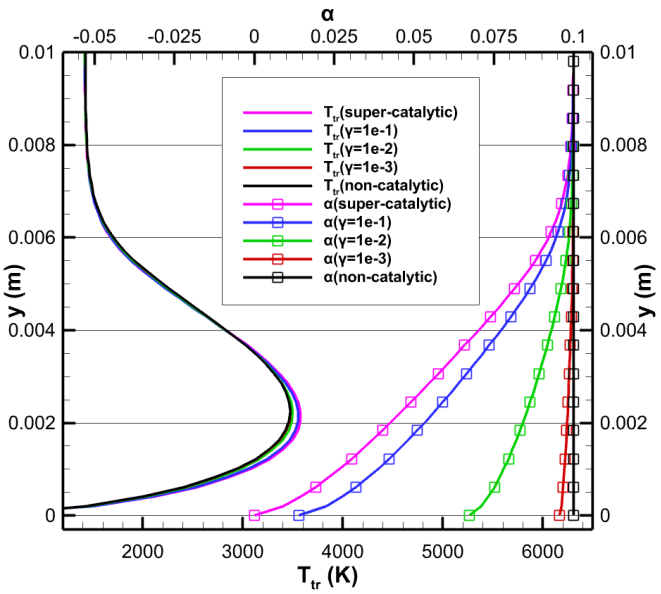

Fig 6. Translational–rotational temperature and degree of dissociation profiles normal to the wall with different catalytic coefficients at $\mathrm{x} = 0.15\mathrm{m}$ in D1 cases.

To verify that the degree of dissociation on the wall is predicted reasonably, the numerical results and Eq. (13) are compared in Fig 7, where scatter points denote the corresponding data taken from position x=0.15m on the flat plate. Good agreement between the numerical results and Eq. (13) can be observed.

Therefore, it is rational to use Eq. (15) to predict $\mathrm{Da_c}$ in characterizing the catalysis nonequilibrium.

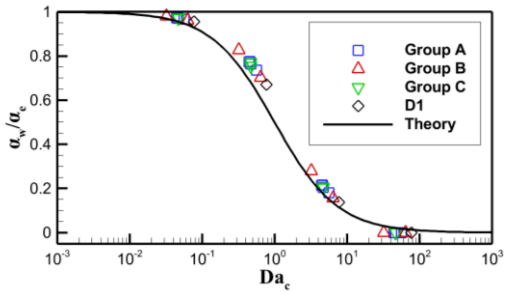

Fig 7. Comparison of numerically simulated dissociation degree of the gas molecules at the wall and predicted values given by Eq. 13

For different free-stream Mach numbers (Group A), different Reynolds numbers (Group B), different degree of dissociation (Group C), and the original real shock tunnel condition (Group D), the numerical results and Eq. (20) predicted results are compared in Fig 8(a), (b), (c), (d), respectively. Good agreement between the numerical results and Eq. (20) can be observed confirming the effectiveness of this equation. Based on the data presented in Fig 8, several observations regarding the impact of surface catalysis and freestream dissociation level can be inferred. Firstly, as the Mach number escalates, there is a decline in the non-dimensional catalytic heating. This phenomenon is attributed to the increase of translational heat transfer, which escalates with the freestream velocity. Secondly, as the Reynolds number rises, there is a slight increase in the non-dimensional catalytic heating ($\mathrm{q_c/q_{tr}}$). This is primarily due to the augmentation of freestream density accompanying the increase in Reynolds number, consequently resulting in a higher $\mathrm{q_c/q_{tr}}$. Thirdly, an elevation in the degree of freestream dissociation leads to an approximately twofold discrepancy in $\mathrm{q_c/q_{tr}}$, maintaining a constant wall catalytic coefficient γ_{cat}. Moreover, within the freestream conditions in an actual experiment (D1), the $\mathrm{q_c/q_{tr}}$ exhibits the potential to double as γ_{cat} spans from 0.01 to 1.

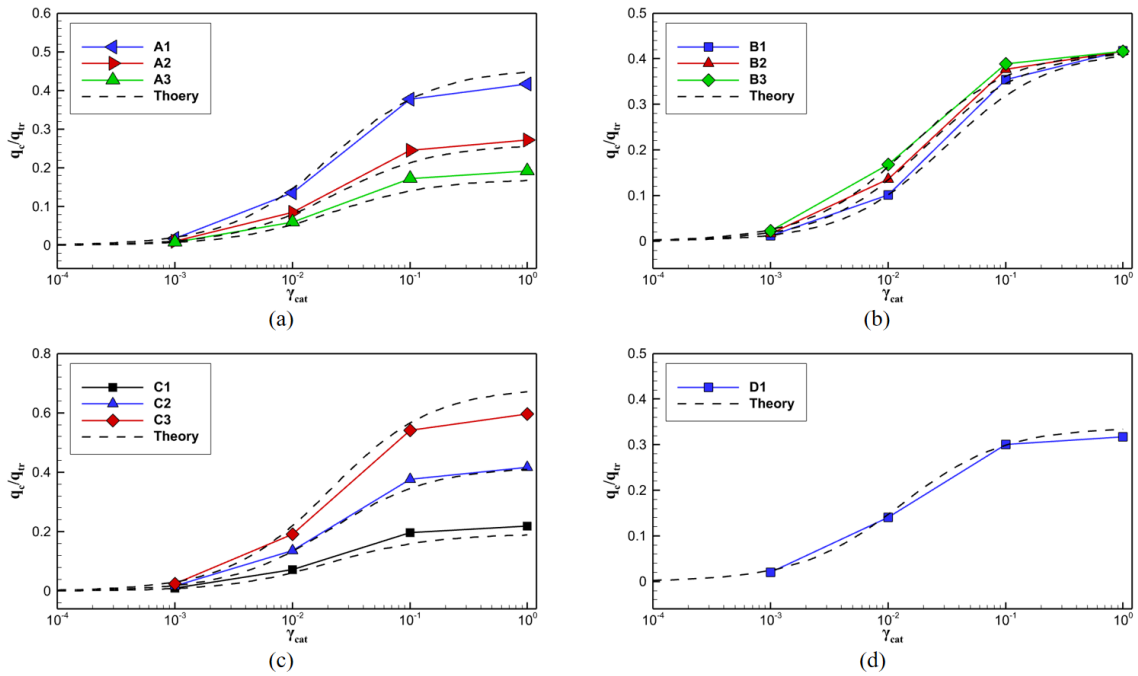

Fig 8. Non-dimensional heat flux to the wall: comparison between numerical results and predicted results using Eq. (20) at x=0.15m: (a) Group A, (b) Group B, (c) Group C, (d) Group D.

5. Conclusions

This study presents theoretical results and numerical simulations aimed at exploring the impact of nonequilibrium catalysis on heat transfer to a flat plate in partially dissociated hypersonic flows. We We

specifically investigate Reynolds numbers within laminar region (10^4~10^5) and medium-to-high Mach numbers (8~12). Initially, our analysis demonstrates that the effects of VT energy transfer and gas phase recombination can be disregarded due to their relatively short characteristic time compared to other processes. Consequently, we found that q_c is independent from q_{tr} and q_v. Subsequently, we introduced a criterion to characterize the nonequilibrium degree of the heterogeneous reactions. Based on this criterion, we derive a formula to predict the aero-heating performance of the flat plate in partially dissociated flows.

The prevalence of nonequilibrium flow in shock tunnel experiments underscores its significance, attracting considerable attention. It is imperative to consider the influence of incomplete catalysis on heat flux measurements in these experiments. The theoretical insights acquired from our study offer valuable guidance for experimental investigations and facilitate the ground-to-flight extrapolation.

References

1. M. Holden: Experimental Studies in the LENS Shock Tunnel and Expansion Tunnel to Examine Real-Gas Effects in Hypervelocity Flows. (2004). https://doi.org/10.2514/6.2004-916
2. Y.-L. Yu, X.-D. Li, Z.-H. Wang, L. Bao: Theoretical modeling of heat transfer to flat plate under vibrational excitation freestream conditions. Int. J. Heat Mass Transf. (2020). https://doi.org/10.1016/j.ijheatmasstransfer.2020.119434
3. M. S. Holden, T. P. Wadhams, M. G. MacLean, A. T. Dufrene: Measurements of Real Gas Effects on Regions of Laminar Shock Wave/Boundary Layer Interaction in Hypervelocity Flows for "Blind' Code Validation Studies. (2013). https://doi.org/10.2514/6.2013-2837
4. G. V. Candler: Rate effects in hypersonic flows. ANNU REV FLUID MECH. (2019). https://doi.org/10.1146/annurev-fluid-010518-040258
5. M. MacLean, M. Holden: Assessment of aerothermal heating augmentation attributed to surface catalysis in high enthalpy shock tunnel flows, Proceedings of the 6th European Symposium on Aerothermodynamics for Space Vehicles 659 (2009). 115–. European Space Agency Paper SP-659.
6. F. R. Van Driest: Investigation of laminar boundary layer in compressible fluids using the crocco method. Technical Report Archive & Image Library (1952). NACA TN 2597
7. N. J.Sliski.: An analytical and experimental investigation of hypersonic viscous interaction pressure effects, Technical Report Archive & Image Library (1973). Report TR-73-58
8. H. Hornung, R. Gollan, P. Jacobs: Computational analysis of experiments on shock detachment in hypersonic flow of nitrogen and carbon dioxide over a wedge. JFM. (2022). https://doi.org/10.1017/jfm.2022.838.
9. G. A. Bird.: Molecular gas dynamics, Oxford University Press. (1976)
10. W. G. Vincenti, C. H. Kruger.: Introduction to physical gas dynamics. Wiley. (1965)
11. J. D. Anderson Jr.: Hypersonic and High-Temperature Gas Dynamics, Second Edition, AIAA Education Series. AIAA Inc., Reston, Virginia. (2006)
12. C. Park.: Review of chemical-kinetic problems of future nasa missions. i - earth entries. J Thermophys Heat Trans. (1993). https://doi.org/10.2514/3.431.
13. WANG Z H, YU Y L, BAO L.: Heat Transfer in Nonequilibrium Flows with Homogeneous and Heterogeneous Recombination Reactions. AIAA J. 56(9), 3593-3599. (2018). DOI:10.2514/1.J056953.
14. Goulard, R.: On Catalytic Recombination Rates in Hypersonic Stagnation Heat Transfer. Journal of Jet Propulsion. 28(11), 737–745. (1958). doi:10.2514/8.7444
15. J. A. FAY, N. H. KEMP, Theory of stagnation-point heat transfer in a partially ionized diatomic gas. AIAA J. 1, 2741–2751. (1963). doi:10.2514/3.2168
16. Zhao Z, Zhang LP, He L, et al.: PHengLEI: a large scale parallel CFD framework for arbitrary

grids. Chin J Comput. 42(11), 2368–83 (2019). https://doi.org/10.11897/SP.J.1016.2019.02368

17. Zhao Z, He L, He XY, et al.: Design of general CFD software PHengLEI. Comput Eng Sci. 42(2), 210–9 (2020). https://doi.org/10.3969/j.issn.1007-130X.2020.02.004.
18. Peng Li, et al. A multi-stage coupling adaptive method for thermochemical nonequilibrium gas. Computers & Fluids. 261, 105916 (2023).
19. Li P, Chen J Q, Ding M S, et al.: Framework design of NNW-HyFLOW hypersonic flow simulation software. Acta Aeronautica et Astronautica Sinica. 42(9), 625718 (2021).
20. CHEN J Q, DING M S, et al.: Simulation of aerothermal effects on reentry capsule geometry in LENS wind tunnel tests. Acta Aeronautica et Astronautica Sinica. 42(S1), 726400 (2021).
21. Matthew MacLean, et al.: Effect of Surface Catalysis on Measured Heat Transfer in Expansion Tunnel Facility. Journal of Spacecraft and Rockets. 50(2), 470-475 (2013)
22. P. Papadopoulos, E. Venkatapathy, D. Prabhu, M.P. Loomis, D. Olynick.: Current grid-generation strategies and future requirements in hypersonic vehicle design, analysis and testing. Appl. Math. Model. 23, 705–735(1999)